The Role of Molecular State and Orientation in Harpooning Reactions: N_2O on Cs/Pt(111)

M. Brandt,[1] T. Greber,[2] N. Böwering,[1] and U. Heinzmann[1]
[1]*Fakultät für Physik, Universität Bielefeld, D-33501 Bielefeld, Germany*
[2]*Physik Institut der Universität Zürich, Winterthurerstrasse 190, CH-8057 Zürich, Switzerland*
(Received 16 June 1997)

The interaction of a beam of state selected and oriented N_2O molecules with 1 ML of Cs on Pt(111) is studied by means of exoelectron emission. While the immediate emission is absent for the impact of ground-state molecules it is present when the molecules are in the first excited $n_2 = 1$ vibrational bending mode. The observed orientational anisotropy agrees with a theory that includes the molecular orientation. The results can be explained in a picture where N_2O approaches the surface with the O end and where—after harpooning—an exoelectron is emitted. [S0031-9007(98)07048-3]

PACS numbers: 79.75.+g, 34.50.Dy

In chemical reactions it is of prime interest to know the intermediate velocities or "effective temperatures" of reaction products. In gas surface reactions exoemission provides experimental access to these quantities. Exoelectron emission reflects a nonadiabatic deexcitation of the chemisorbing molecule where energies exceeding the work function are released in a single charge transfer process. The generally accepted mechanism for this emission comprises the Auger deexcitation of a molecular hole–state at energies below the Fermi level [1–3]. The dynamics of this hole injection process strongly influences the yield of exoelectrons. If the molecule approaches the surface with thermal energies, the electronic system manages to stay in equilibrium with the nuclear coordinates and the heat of adsorption is dissipated adiabatically. If, however, "harpooning" occurs, i.e., if the impinging molecule becomes resonantly ionized and is accelerated in the image field, further charge transfer may proceed on nonequilibrium potential energy surfaces [4,5]. Any subsequent charge transfer may then proceed under the emission of an exoelectron. The difference between the ionization potential of the surface and the vertical electron affinity of the molecule determines the harpooning distance and the corresponding acceleration of the ions [5]. The vertical electron affinity is the energy difference between the lowest unoccupied and the highest occupied molecular orbital in the uncharged state [6,7]. For diatomic molecules like oxygen [8,9] or chlorine [6,10], the corresponding reaction models have been derived. It was argued that the orientation of the molecule relative to the surface normal should influence the dissociation dynamics and thus the exoemisson yield [6,11]. In this Letter, we report experimental evidence for a strong orientational dependence of the exoelectron yield. Here the interaction of nitrous oxide (N_2O) with Cs is studied. In the first excited vibrational state the linear molecule (NNO) may be oriented by means of the Stark effect. It turns out that the exoelectron yield from the reaction of oriented N_2O approaching a Cs-covered Pt(111) surface with the oxygen end is strongly enhanced in comparison to randomly oriented N_2O. Furthermore, the excited vibrational state in the $n_2 = 1$ bending mode is much more exoactive than the molecular ground state of N_2O.

The experiments were performed with a molecular beam apparatus [12,13] that was adapted for the state selection and orientation of N_2O and the detection of low-energy electrons. Figure 1 shows a schematic diagram of the experimental setup. The base pressure in the sample chamber was below 1×10^{-10} mbar. Cs was evaporated on Pt(111) from SAES getter sources. The coverage of 1 ML of Cs was prepared by heating the sample above the multilayer desorption temperature of 300 K. The monolayer Cs is reflected in a $(\sqrt{3} \times \sqrt{3})R30°$ LEED pattern. During the experiments, the sample was kept at 150 K.

At a repetition rate of 60 Hz the seeded molecular beam produces N_2O pulses with a duration of 0.5 ms FWHM on the sample. The N_2O flux is measured with a mass spectrometer in the analysis chamber. At a nozzle y temperature of 470 K the N_2O translational velocity is 900 m/s. The angle of incidence is 30° with respect to the surface normal. The N_2O beam is state selected in the $|J, l, M\rangle = |111\rangle$ rotational state of the $n_2 = 1$ bending vibration ($\hbar\omega_2 = 73$ meV) [14] by means of an electrostatic hexapole field [15]. The degree of orientation of the $N_2O|111\rangle$ molecules can be varied by changing the orientation field in front of the sample. Low-energy electrons can be collected only by the detector for one polarity of the orientation field. This allows isotropic (low field) and preferentially O-end approach (high field) to the surface

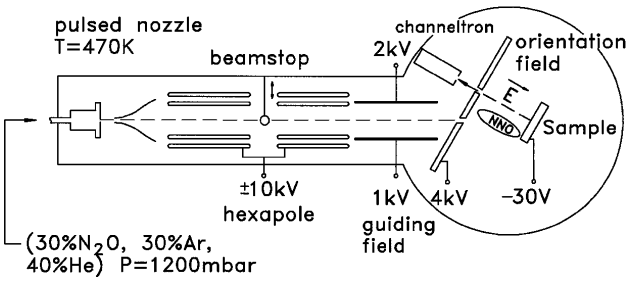

FIG. 1. Schematic diagram of the experimental apparatus.

 0031-9007/98/81(11)/2376(4)$15.00

[16]. We define the orientational anisotropy as $A_{\text{exp}} \equiv (Y_{\text{O-end}} - Y_{\text{unoriented}})/(Y_{\text{O-end}} + Y_{\text{unoriented}})$ where Y is the exoelectron yield for the corresponding configuration. A_{exp} rises as a function of the orientation field strength and quantitatively follows the Stark coupling behavior of $N_2O|111\rangle$ [15] that saturates for orientation fields above 2 kV/cm.

The electron emission is measured with a channeltron in normal emission. The transmission of the detector is calibrated by means of photoelectrons excited by laser light which is collinear to the molecular beam. The channeltron feeds two counters, A and B. While counter A records the total charge, counter B registers the emission that coincides within a gate of 1 ms with the arrival of the gas pulse on the surface. The detector does not discriminate between electrons and negative ions. However, in contrast to the O_2 + Cs reaction where O^- ion emission is observed [17] we do not expect O^- emission from the $N_2O + Cs \rightarrow O^- + N_2 + Cs$ reaction since it is endothermic by $\sim$2.3 eV.

In a first set of experiments a flux of N_2O with a variable fraction of molecules in the ($n_2 = 1$) state is prepared. The orientation field is switched off and hence the molecules strike the surface unoriented. The beam stop is removed and the hexapole voltage is switched in a sequential mode every 10 s from $\pm$10 kV to 0 V. Consequently, the fraction of the N_2O ($n_2 = 1$) molecules varies. We estimate the portion of vibrationally excited N_2O molecules in the focused beam to be 2.4 times higher than in the unfocused beam. Figure 2 shows the exoelectron yield from the reaction of N_2O with 1 ML Cs on Pt(111) for unselected molecules (unfocused) and for $n_2 = 1$ vibrational state-enriched molecules (focused) as a function of time. The yield corresponds to the exoelectron current normalized with the N_2O flux. The delayed emission (counter A – counter B) is not immediately related with the adsorption process and indicates the deexcitation of metastable precursor states. For the case of O_2 + Cs such exoemission has been found and identified as being related to the dissociation of a metastable O_2^- species on the surface [18,19]. As can be seen from Fig. 2a the delayed emission is almost unaffected by the state composition of the N_2O beam. Here, the details in the kinetics of the delayed emission will not be discussed. In contrast to the delayed emission, the immediate emission (channel B) (see Fig. 2b) strongly depends on the state composition of the impinging N_2O beam. For the following, the emission from a clean surface ($t = 0$ s) shall be considered since it is expected that there all molecules meet the same surface conditions. At the beginning of the reaction the sticking coefficient as determined by the King and Wells method [20] is found to be close to unity for both beam conditions. The ratio between the exoelectron emission for the enriched (focused) and the thermal (unfocused) beam is 2.3 $\pm$ 0.2 and corresponds within the error bars to the ($n_2 = 1$) ratio of 2.4 in the two beams. Therefore, it is concluded that only excited N_2O molecules cause immediate exoemission. A key to

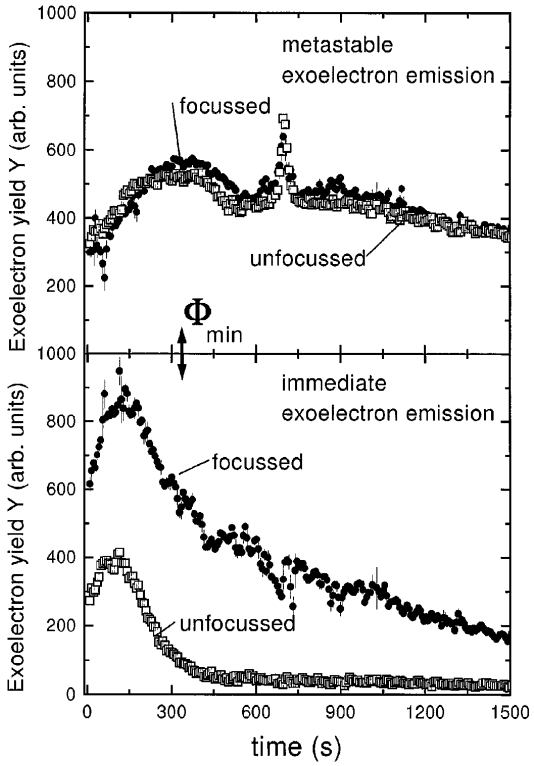

FIG. 2. Exoelectron yield during the oxidation of Cs on Pt(111) with a pulsed focused and unfocused N_2O beam. In the upper diagram the exoemission not coinciding with the gas pulse, related to the deexcitation of a metastable species, is shown as a function of time and molecular state. The lower diagram shows the exoemission during the impact of N_2O molecules on the surface. This immediate emission scales with the fraction of vibrationally excited N_2O molecules. The arrows indicate the position of the work-function minimum that was found from photoemission yield measurements.

the interpretation of this result can be obtained from gas phase experiments where the dissociation cross sections induced by electron attachment ($N_2O + e^- \rightarrow N_2 + O^-$) were found to depend strongly on the gas temperature. By increasing T from 350 to 1000 K Chantry found an increase of the cross section of this reaction with thermal electrons by 3 orders of magnitude [21]. This dramatic effect is related to the fact that the vertical electron affinity of N_2O is lowered from -2.2 eV in the ground state to -1.5 eV in the $n_2 = 1$ state since the bending mode configuration is closer to that of the bent N_2O^- ion [22]. For the case of the chemisorption of N_2O on Cs this indicates that the electron affinity of the linear ground state is too low for harpooning in the incident trajectory and that therefore no Coulomb acceleration takes place as it does in the vibrationally excited state.

In a second set of experiments the beam stop blocks the direct molecular beam and the hexapole focuses only vibrationally excited N_2O molecules which are predominantly in the $|111\rangle$ state. In these experiments the orientation field is switched in a sequential mode during the experimental run every 10 s from 2 kV/cm (oriented) to 0.03 kV/cm

(unoriented). In the upper part of Fig. 3 the immediate exoelectron yields (counter B) from the exposure of oriented and unoriented N_2O molecules are shown as a function of time. Here the exoelectron current is normalized with the detector transmission function which is orientation field dependent. An initial orientational anisotropy A_{exp} of 0.45 ± 0.05 for the immediate exoelectrons is found. The anisotropy decreases exponentially from the maximum at the beginning of the oxidation (see lower part of Fig. 3). It is worth noting that there is no measurable anisotropy A_{exp} in the delayed emission. The measured anisotropy of 0.45 is close to the theoretical upper limit of 0.5 for the orientational anisotropy of the $|111\rangle$ state [23]. The difference might be caused by incomplete orientation in the high field and/or residual orientation in the low field configuration. In the following, however, a model is presented that lowers the maximum orientational anisotropy due to the circumstance that not only normally incident molecules may cause exoemission.

The orientational anisotropy is a sensitive observable for the test of theories for nonadiabatic adsorption processes that are associated with particle emission. The nonadiabatic yield is proportional to $\exp(-\nu^\star/\nu)$ where $\nu^\star$ is a characteristic velocity that describes the dynamics of the excitation/deexcitation process and where ν is the relative velocity of the reacting particles [24]. This law was applied in several studies where the velocity of the impinging molecules was varied [6,11,25]. The $\nu^\star$ values that are in the order of 10^4 m/s, can be calculated from theories that describe nonadiabatic charge transfer [3,6,11,24]. To determine $\nu^\star$ values from the experiment it has to be considered that the molecule is accelerated after harpooning. Therefore, $\nu = \alpha(\nu_\perp + \nu_c)$ appropriately describes the velocity of the particles in the process that is accompanied by exoemission. $\nu_\perp$ is the initial normal velocity component, ν_c the velocity due to the Coulomb acceleration, and α is an "efficiency number" that is ≤ 2 for the case of O_2 + Cs [11]. If the initial orientation of the molecule plays a role, the efficiency

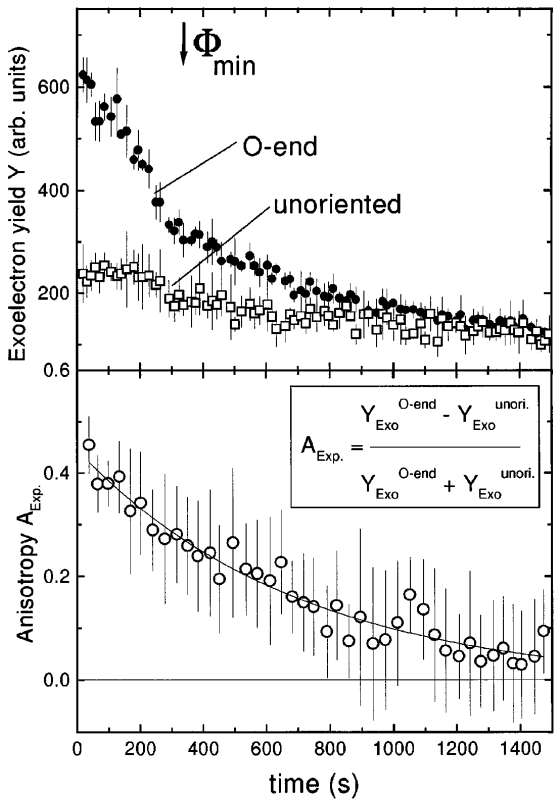

FIG. 3. Upper part: Immediate exoemisson during the oxidation of Cs/Pt(111) with O-end oriented N_2O and for unoriented $N_2O|111\rangle$ molecules as a function of time. The arrow indicates the position of the work-function minimum. Lower part: Corresponding exoemission orientation anisotropy.

number may be rewritten as $\alpha = \beta\cos(\theta)$ where $\cos(\theta)$ is the projection of the molecular axis on the surface normal, and where β describes the coupling of momentum to the reaction coordinate. Now the orientational anisotropy A_{theor} may be calculated from the integral of the $\exp(-\nu^\star/\nu)$ factors that are weighted with the orientational probability distribution functions $P_{|111\rangle}$ and $P_{|\text{iso}\rangle}$ [23] of the states under investigation:

$$P_{\text{exo}}^{\text{O-end}} \propto \int_0^{\pi/2} \exp\left[-\frac{\nu^\star}{|\cos(\Theta)|\beta(\nu_\perp + \nu_c)}\right] P_{|111\rangle}(\Theta)\sin(\Theta)\,d\Theta\,,$$

$$P_{\text{exo}}^{\text{unori}} \propto \int_0^{\pi/2} \exp\left[-\frac{\nu^\star}{|\cos(\Theta)|\beta(\nu_\perp + \nu_c)}\right] P_{|\text{iso}\rangle}(\Theta)\sin(\Theta)\,d\Theta\,,$$

$$\langle A_{\text{theor}}^{\text{O-end}}\rangle = (P_{\text{exo}}^{\text{O-end}} - P_{\text{exo}}^{\text{unori}})/(P_{\text{exo}}^{\text{O-end}} + P_{\text{exo}}^{\text{unori}})\,. \quad (1)$$

Here $P_{\text{exo}}^{\text{O-end}}$ and $P_{\text{exo}}^{\text{unori}}$ denote the probabilities for the exoelectron emission for preferential O-end collisions and for the unoriented case, respectively. $P_{|111\rangle}$ and $P_{|\text{iso}\rangle}$ represent the normalized orientational probability density functions for the oriented $|111\rangle$ and the unoriented, i.e., isotropic $|111\rangle$ state, respectively [23]. It turns out that the $\langle A_{\text{theor}}^{\text{O-end}}\rangle$ values are constant in a wide range of $\nu^\star/\beta\nu = 10 \pm 5$ values. This implies that only the order of magnitude of the $\nu^\star$ values has to be known for the determination of the orientation that triggers exoemission. We find $\langle A_{\text{theor}}^{\text{O-end}}\rangle = 0.47$ for O-end N_2O collisions being exoactive, 0.15 for both ends active, and -0.99 for N-end approach. The comparison with the experimental $A_{\text{exp}} = 0.45$ value supports a picture where only the O-end approach causes exoelectron emission. From these findings we can derive a model for the exoemission process in the N_2O + Cs case. Figure 4 shows a schematic diagram. N_2O approaches the surface, becomes

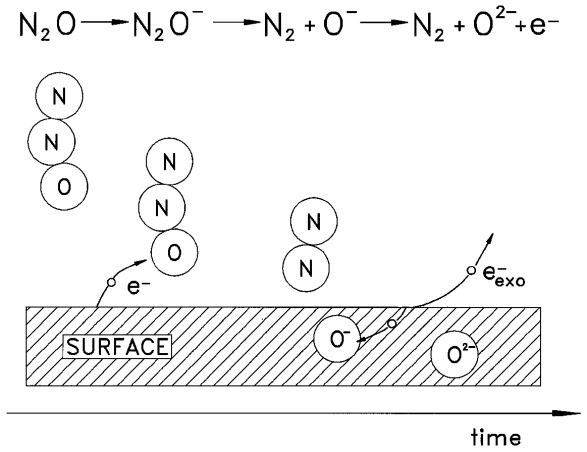

FIG. 4. Model for harpooning and direct dissociation for N_2O on Cs/Pt(111). The molecules approach the surface adiabatically and are resonantly ionized (harpooned). The molecules accelerate and dissociate. The highly excited O^- dissociation intermediates may be nonadiabatically deexcited by the emission of exoelectrons.

resonantly ionized (harpooned), accelerates, and starts to dissociate into $N_2 + O^-$. If the dissociation is fast enough the hole on the O^- $2p^5$ ion may dive to energy levels deeper than the work function and deexcite via the emission of an Auger electron from the substrate in the closed-shell O^{2-}-like ground state [3,8,9]. Apparently, the vertical electron affinity and the molecular orientation strongly affect the dynamics of the adsorption process. From the analysis of the exoemisson yield it is concluded that in an unfavorable normal molecular axis adsorption geometry the intermediate kinetic energies, i.e., the effective temperatures, are largest in the dissociation products. As indicated by the "absence" of exoemission from N_2O ground-state molecules for the interaction with Cs ($\Phi_{Cs} = 2$ eV) the difference between the work function and the vertical affinity of N_2O, $\Phi - E_A^V(n_2 = 0)$ of 4.2 eV is too large in order to initiate harpooning. On the other hand, the exoemission from state-selected N_2O ($n_2 = 1$) indicates that at metallic surfaces harpooning still occurs for $\Phi - E_A^V(n_2 = 1) = 3.5$ eV. It is rather surprising that such a large down-shift of the affinity level may occur. It links, however, the present results with those of Brune *et al.* [26] who found after the dissociative adsorption of oxygen on Al oxygen adatoms that are separated by more than 80 Å. These findings are not compatible with energy dissipation theories and a dissociation pathway parallel to the surface [27]. However, experiment and theory can be reconciled with an uncommon dissociation process—normal to the surface—that leads to ballistic oxygen motion. From the present findings of the N_2O + Cs reaction it can be concluded that also for the case of O_2/Al(111) the difference $\Phi - E_A^V$ is in the range where harpooning may be effective and where a dissociation normal to the surface becomes plausible. In conclusion, it was shown that exoemission experiments with state-selected and oriented molecules contribute to a better understanding of the stereodynamics of chemisorption and harpooning reactions at surfaces.

For T. G. it is a pleasure to acknowledge the hospitality and fruitful research atmosphere at ZIF and the faculty of Physics at the University of Bielefeld. This work was financially supported by the DFG (SFB 216) and the ZIF-project: "interaction of oriented molecules."

[1] T. F. Gesell, E. T. Arakawa, and T. A. Callcott, Surf. Sci. **20**, 174 (1970).
[2] B. Kasemo, E. Törnqvist, J. K. Nørskov, and B. I. Lundqvist, Surf. Sci. **89**, 554 (1979).
[3] T. Greber, Chem. Phys. Lett. **222**, 292 (1994).
[4] J. W. Gadzuk, Comments At. Mol. Phys. **16**, 219 (1985).
[5] T. Greber, Surf. Sci. Rep. **28**, 1 (1997).
[6] L. Hellberg, J. Strömquist, B. Kasemo, and B. I. Lundqvist, Phys. Rev. Lett. **74**, 4742 (1995).
[7] J. L. Magee, J. Chem. Phys. **8**, 687 (1940).
[8] K. Hermann, K. Freihube, T. Greber, A. Böttcher, R. Grobecker, D. Fick, and G. Ertl, Surf. Sci. **313**, L806 (1994).
[9] T. Greber, K. Freihube, R. Grobecker, A. Böttcher, K. Hermann, G. Ertl, and D. Fick, Phys. Rev. B **50**, 8755 (1994).
[10] B. Kasemo, Surf. Sci. **363**, 22 (1996).
[11] T. Greber, A. Morgante, S. Fichtner-Endruschat, and G. Ertl, Surf. Rev. Lett. **2**, 273 (1995).
[12] G. H. Fecher, N. Böwering, M. Volkmer, B. Pawlitzky, and U. Heinzmann, Vacuum **41**, 265 (1990).
[13] M. Brandt, H. Müller, G. Zagatta, O. Wehmeyer, N. Böwering, and U. Heinzmann, Surf. Sci. **331–333**, 30 (1994).
[14] D. G. Hopper, A. C. Wahl, R. L. C. Wu, and T. O. Tiernan, J. Chem. Phys. **65**, 5474 (1976).
[15] D. H. Parker, H. Jalink, and S. Stolte, J. Phys. Chem. **91**, 5427 (1987).
[16] H. Jalink, D. H. Parker, and S. Stolte, J. Mol. Spectrosc. **121**, 236 (1987).
[17] T. Greber, R. Grobecker, A. Morgante, A. Böttcher, and G. Ertl, Chem. Phys. Lett. **70**, 1331 (1993).
[18] R. Grobecker, H. Shi, H. Bludau, T. Hertel, T. Greber, A. Böttcher, K. Jacobi, and G. Ertl, Phys. Rev. Lett. **72**, 578 (1994).
[19] R. Grobecker, T. Greber, A. Böttcher, and G. Ertl, Phys. Status Solidi (a) **146**, 119 (1994).
[20] D. A. King and M. G. Wells, Surf. Sci. **29**, 454 (1972).
[21] P. J. Chantry, J. Chem. Phys. **51**, 3369 (1969).
[22] D. J. Wren and M. Menzinger, Discuss. Faraday Soc. **67**, 97 (1979).
[23] S. E. Choi and R. B. Bernstein, J. Chem. Phys. **85**, 150 (1986).
[24] G. Blaise and A. Nourtier, Surf. Sci. **90**, 495 (1979).
[25] A. Böttcher, A. Morgante, T. Gießel, T. Greber, and G. Ertl, Chem. Phys. Lett. **231**, 119 (1994).
[26] H. Brune, J. Wintterlin, R. J. Behm, and G. Ertl, Phys. Rev. Lett. **68**, 624 (1992).
[27] J. Jacobsen, B. Hammer, K. W. Jacobsen, and J. K. Nørskov, Phys. Rev. B **52**, 14 954 (1995).